Determination of Longitudinal and Transverse Behaviour of Continuous Fibre-Reinforced Composites from Vee-Bending

R.J. Dykes, T.A. Martin, D. Bhattacharyya
Composites Research Group, Mechanical Engineering Department, University of Auckland, Private Bag 92019, Auckland, New Zealand.

Abstract

Single curvature bending of fibre reinforced thermoplastic (FRTP) composites has been demonstrated to be a useful method for determining the longitudinal shear behaviour of these materials. This paper further examines the vee-bending method as a means of analysing the transverse shear response of a glass fibre-reinforced polypropylene material. Laminated strips, with layers possessing reinforcing fibres aligned either parallel or perpendicular to the bend axis, are subjected to a novel bending operation between two highly polished platens, designed in such a way as to ensure a constant rate of shear deformation. Interpretation of the material's longitudinal and transverse behaviour is made by way of an idealised fibre-reinforced material (IFRM) model subject to the kinematic constraints of incompressibility and fibre inextensibility. The experiments demonstrate the suitability of the method for comparing the transverse and longitudinal shear behaviour of such materials.

Introduction

Fibre reinforced thermoplastic (FRTP) materials have enjoyed a steady rise in popularity over recent times which can be largely attributed to the way in which they lend themselves to rapid processing applications[1]. Their ability to be quickly formed into fairly complex 3-dimensional components from sheet stock by the application of heat and relatively low forces seems to have broadened their appeal to a widening number of manufacturers. Of additional benefit is the abundance of processing methods now available for FRTP materials, a large proportion of which have been derived from existing sheet metal forming operations.

The rapid advances made in the field of manufacturing technology have perhaps intensified the need to establish more reliable methods of characterising and

determining the thermo-rheological behaviour of such materials. There is now a well established theory[2] describing the deformation of continuous FRTPs, the simplest of which assumes the composite to possess inextensible fibres embedded within an incompressible viscous medium. The theory leads to the recognition of two important material parameters; namely the longitudinal shear, η_L, and transverse shear, η_T, viscosities. These two parameters govern the stress in the composite body and hence they must be determined by means of experiment.

To date, efforts in determining η_L and η_T have focused on variations of ply pull-out[3] and oscillatory shear experiments[4], both of which provide useful information regarding the behaviour of such materials. More recently however, a novel way of isolating and studying the longitudinal shear behaviour of continuous fibre reinforced thermoplastic composites has been proposed by Martin *et al.*[5] who obtained a solution for the three point bending of an ideal viscous beam using an IFRM model. Unfortunately, the solution failed to match the experimentally observed behaviour of the glass fibre/PP laminates. Mander[6] subsequently imposed further constraints on the deformation using a vee-bending jig which had two polished platens to "wrap" the laminate around the roller minimising any indentation tendency commonly found in vee-bending tests. This allowed the true longitudinal shear response of the material to be determined. This paper further examines this novel vee-bending method by employing a cam profile to keep the shear deformation rate constant and establishes its usefulness as a means of establishing both the longitudinal and transverse shear behaviour of continuous FRTPs such as PLYTRON® (a glass fibre/PP composite, originally developed by ICI Ltd. UK).

Development of a Laminated Viscous Beam Model

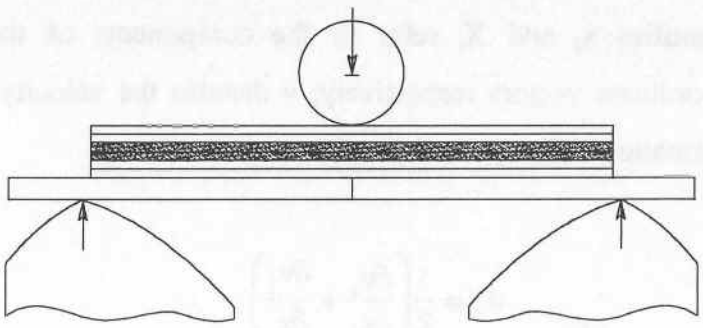

Figure 1. Vee-bending of a laminated viscous beam.

Thermoplastic polymers are generally known to exhibit viscous behaviour at temperatures within or above their molten temperature ranges. The matrix material in reinforced thermoplastic composites can therefore be idealised as an incompressible Newtonian fluid in its molten state. In addition, there is the added constraint that the fibres impose on the composite body. In the case of continuous fibre reinforced thermoplastics, the fibres may be thought of as homogeneously distributed inextensible cords. In this part of the paper, we consider the plane strain bending of an initially flat laminated beam as illustrated in Figure 1. The analysis is limited to the case in which the fibres of the individual layers are restricted to lie either in the plane of deformation, or orthogonal to it as shown in Figure 1. Further limitations of the theory will be discussed later on. Some of the equations presented in the following analysis may be found in Spencer's[2] text but are repeated to maintain the comprehensiveness of the theoretical approach.

Kinematic Constraint Conditions

Let us first consider the kinematic constraints placed upon a body due to the assumptions of incompressibility and fibre inextensibility. In the following analysis capital letters are used to indicate vector quantities referred to the reference state while lower case letters are used to indicate vector quantities in the deformed state. The incompressibility constraint condition may be written mathematically as

$$\frac{\partial v_i}{\partial x_i} = d_{ii} = 0 \qquad (1)$$

where the quantities x_i and X_i refer to the components of the deformed and undeformed coordinate vectors respectively; $\mathbf{v}$ denotes the velocity vector; and $\mathbf{d}$ is the rate of deformation tensor given by

$$d_{ij} = \frac{1}{2}\left(\frac{\partial v_i}{\partial x_j} + \frac{\partial v_j}{\partial x_i}\right) \qquad (2)$$

A family of fibres in the undeformed configuration may be represented by a field of unit tangent vectors $A(X_R)$. The directions of the fibres at any particle in the continuum are then given by **A**. Therefore, the trajectories of **A** represent the fibres themselves and the components of **A** are denoted by A_R. During deformation the fibres are convected with the continuum and the same particles will lie on a given fibre at any time. The fibre paths in the deformed state may then be represented by the trajectories of a new unit vector field $a(X_R,t)$. Using these definitions the fibre inextensibility condition may be written as

$$a_i a_j \frac{\partial v_i}{\partial x_j} = a_i a_j d_{ij} = 0 \qquad (3)$$

The only other constraint imposed on the deformation is that of plane strain. Pipkin and Rogers[7] have derived the theory for plane strain deformations of incompressible materials where the reinforcement is restricted to lie in the plane of deformation (X_3 = constant). The two main results arising from their analysis indicate that the fibres must remain in parallel surfaces, and that the thickness of the sheet cannot change during any plane strain deformation. It is obvious from these two conditions that the only form of deformation available to such a material under the stipulated conditions is that of simple shear along the direction of the fibres.

We now consider the transversely orientated layers which do not kinematically influence the deformation in the plane, but only serve to enforce the plane strain condition already assumed. We make the assumption that the thickness of these layers remains constant during any plane strain deformation. In other words, it is assumed that the transverse layers exhibit the same kinematic behaviour as the longitudinal layers. By way of an example, consider the shear deformation of an initially flat laminated plate consisting of three layers as shown in Figure 2. The outer two (longitudinal) layers possess fibres which lie in the plane of deformation while the reinforcement in the central (transverse) layer is aligned in the direction of the X_3 axis. The unit vector **b** represents the shearing direction such that **a**.**b** = 1 in the longitudinal layers, and **a**.**b** = 0

in the transverse layer. The unit vector **n** is defined to be orthogonal to both the shearing direction and the X_3 axis. The left hand side of the plate is embedded along the x_2 axis and rigid body rotations and translations have been ignored. The shear strain through the entire plate is therefore constant and may be simply expressed by the angle that the plate makes with the x_1 axis.

$$\gamma = \phi \tag{4}$$

The shear rate $\dot{\gamma}$ can then be simply expressed in terms of ϕ as

$$\dot{\gamma} = \dot{\phi} \tag{5}$$

This result is useful when establishing a constitutive relationship for a viscous fluid.

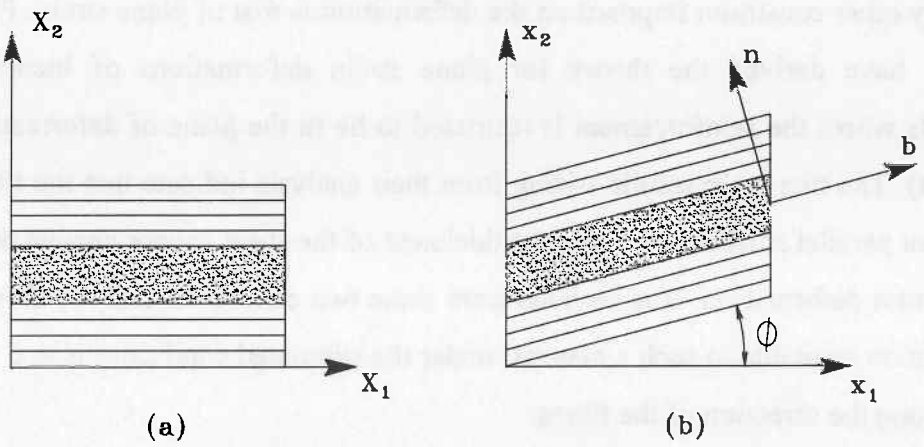

Figure 2. (a) Undeformed plate; (b) Deformed plate.

Stress in a Constrained Material

The total stress in a constrained material can be thought of as the sum of a reaction stress, r_{ij}, and an extra stress S_{ij}.

$$\sigma_{ij} = r_{ij} + S_{ij} = -p(\delta_{ij} - a_i a_j) + T a_i a_j + S_{ij} \tag{6}$$

where S_{ij} satisfies the constraints $b_i b_j S_{ij} = 0$ and $n_i n_j S_{ij} = 0$

In other words, S_{ij} involves no normal stress component on surface elements normal to the **b** or **n** directions. The reaction stress does no work in the deformation and the reactions p and T arise as a result of the incompressibility and inextensibility conditions respectively. T is the total tension on elements normal to the fibre direction and p represents the total pressure on elements normal to the **n** direction. These scalar terms must be determined by solving the equilibrium equations. The deviatoric stress tensor, S_{ij} needs to be specified by an appropriate constitutive relationship. If the material possesses reflectional symmetry in the X_3 plane and the deformation is homogeneous, under plane strain conditions the only non-zero components of σ_{ij} are

$$\sigma_{ij} = -p(\delta_{ij} - a_i a_j) + Ta_i a_j + S(a_i n_j + a_j n_i) + S_{33} k_i k_j \qquad (7)$$

where **k** is the unit vector normal to the plane of deformation. A constitutive relationship is required to define S_{33} and S.

Constitutive Equation

According to Rogers[8], the constitutive relationship for a viscous fluid subject to the stipulated constraints is given by

$$S_{ij} = 2\eta_T d_{ij} + 2(\eta_L - \eta_T)(a_i a_k d_{kj} + a_j a_k d_{ki}) \qquad (8)$$

where η_L and η_T are the respective longitudinal and transverse viscosities of the continuum. In a plane strain deformation $v_3 = d_{33} = 0$. As the fibre directions differ in the longitudinal and transverse layers, it is necessary to consider the stress in both layers separately. The fibre direction in the longitudinal layers coincides with the shearing direction and can be simply specified in component form by

$$\mathbf{a}_L = \mathbf{b} = (\cos\phi,\ \sin\phi,\ 0)$$

Using equations (8) and (7) it can then be shown that

$$S_L = b_i n_j \sigma_{ij} = b_i n_j S_{ij} = 2\eta_L b_i n_j d_{ij} = \eta_L \dot{\gamma} = \eta_L \dot{\phi} \qquad (9)$$

where S_L is the shear stress associated with the simple shear deformation along the fibre, or longitudinal, direction. For the transverse layers the fibre direction coincides with the X_3 direction and may therefore be specified in component form by $\mathbf{a}_T=(0\ 0\ 1)$. Similarly, using the same equations that lead to (9), it can be shown that the shear stress in the transverse layers is given by

$$S_T = b_i n_j \sigma_{ij} = b_i n_j S_{ij} = 2\eta_T b_i n_j d_{ij} = \eta_T \dot{\gamma} = \eta_T \dot{\phi} \qquad (10)$$

For a viscous fluid model the shear stress in either layer only depends on the shear rate and the viscosity. For a laminated strip of material, such as the one described, both the transverse and longitudinal viscosities of the material can be determined from the constitutive equation in the following manner.

Stress Equilibrium

According to equations (9) and (10) the shear stress through a laminated strip varies discontinuously at the boundary surfaces and interfacial surfaces between differently orientated layers. Initially it would appear as though equilibrium between the adjacent layers is therefore unachievable. However there exists the possibility that a sheet of fibres can support a finite force and hence an infinite tension. In the present analysis it is necessary to accommodate discontinuities in S at the outer surfaces of the strip ($\xi = 0$, $\xi = h$) and also at the interfacial surfaces. We may achieve this by using step and delta functions that allow T to take infinite values in the fibres in the material adjacent to the boundary surfaces, and in the fibres adjacent to, and on either side of, interfacial surfaces. The effect of this is to introduce simple jump discontinuities. For further clarification of this property the readers are referred to Rogers and Pipkin [9] where the

discontinuous stress condition is used to satisfy the shear traction boundary conditions in plane strain bending problems. Spencer[10] has also shown how the same property can be used to admit shear stress discontinuities for the more general case in which the individual layers of an elastic laminated beam can assume any orientation oblique to the plane of deformation.

The equilibrium of the deformed plate, shown in Figure 3(a), may be expressed in terms of the hydrostatic pressure and the resultant shear and tensile forces, denoted by S^* and T^* respectively. As illustrated, these resultant forces act on the face normal to the shearing direction and can be simply evaluated by integrating through the thickness of deformed plate. The resultant shear force per unit width can therefore be expressed by

$$S^* = \int_0^{\xi_1} S_L d\xi + \int_{\xi_1}^{\xi_2} S_T d\xi + \int_{\xi_2}^{h} S_L d\xi \qquad (11)$$

where h is the total thickness of the plate. Substitution of equations (9) and (10) into the above equation yields an expression for the resultant shear force per unit width.

$$S^* = \dot{\phi}(h_L \eta_L + h_T \eta_T) \qquad (12)$$

where h_L and h_T represent the total thicknesses of the longitudinal and transverse layers respectively. (ie. $h_L = h - \xi_2 + \xi_1$ and $h_T = \xi_2 - \xi_1$).

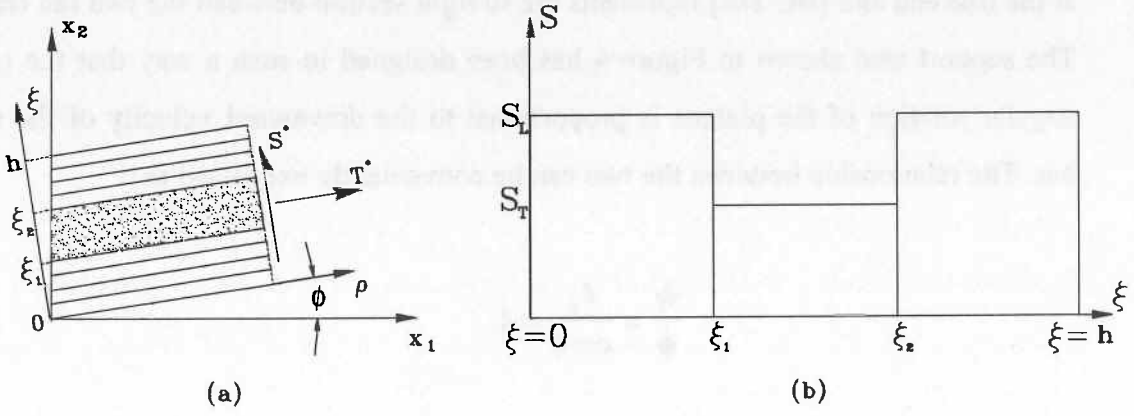

Figure 3. (a) Resultant forces acting on a deformed plate, (b) Shear stress distribution through the thickness of a laminated plate (assuming $\eta_L > \eta_T$).

Kinematic Model for a Vee-bend

The following kinematic solution is proposed for the deformation of a flat laminated plate subjected to the novel bending operation illustrated in Figure 4. Only half the deformed strip is shown as symmetry exists in the (x_2, x_3) plane. A more detailed explanation of the workings of the jig follow later.

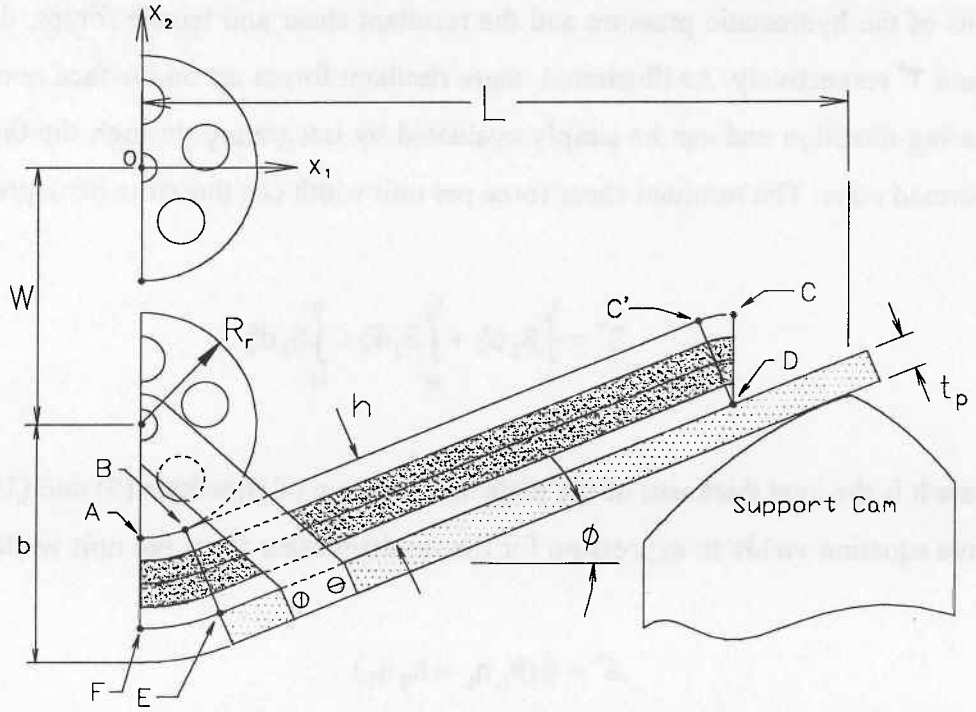

Figure 4. Kinematic vee-bending model (Not to scale).

The half-strip, shown in Figure 4, may be divided into three sections: [ABEF] represents the fan region beneath the radius bar, [CC'D] represents another fan region at the free end and [BC'DE] represents the straight section between the two fan regions. The support cam shown in Figure 4 has been designed in such a way that the rate of angular rotation of the platens is proportional to the downward velocity of the radius bar. The relationship between the two can be conveniently expressed as

$$\frac{\dot{w}}{\dot{\phi}} = \frac{\ell_p}{\cos\phi} = L \qquad (13)$$

where ℓ_p is the orthogonal distance between centre of the radius bar and the point of contact between the platen and the supporting cam. Both ℓ_p and cosϕ vary with w, but the ratio of the two remains constant and equal to L for all ϕ. The kinematic model leads to the result that the shear rate in sections [ABEF] and [CC'D] is zero. Consequently these fan regions move down like rigid bodies and thus the shear stress through these regions is zero. In region [BC'DE] the strip remains straight and the shear rate, $\dot{\gamma}$, is equal to the rate of angular rotation of the platen and strip, $\dot{\phi}$, defined in equation (13).

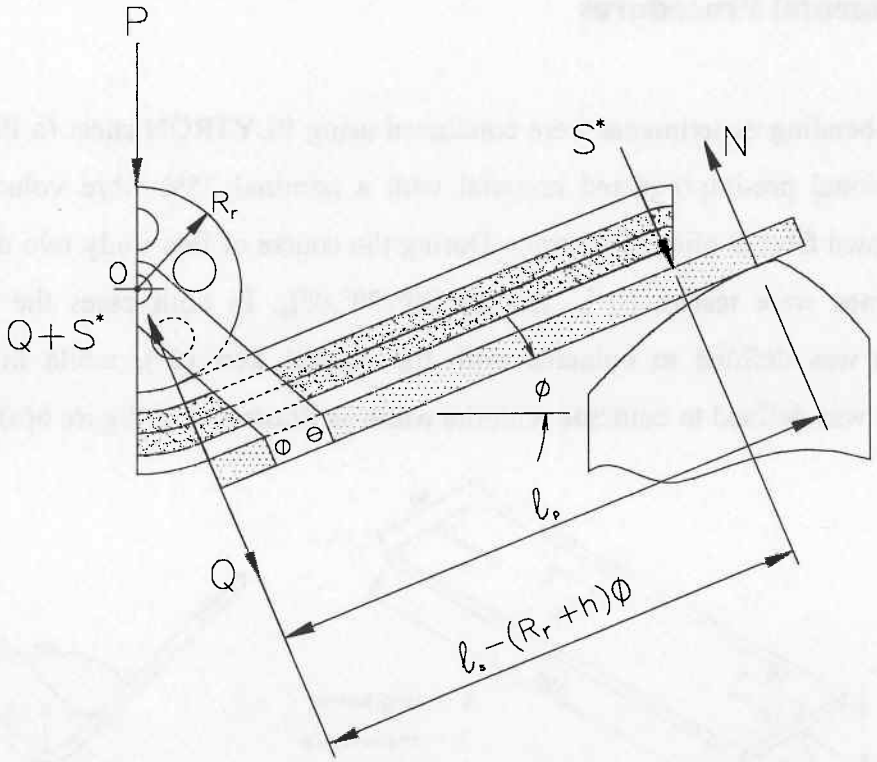

Figure 5. Equilibrium of the vee-bending mechanism.

The net downward load on the radius bar can be calculated by considering the equilibrium of the entire bending mechanism as shown in Figure 5. When the sample is bent to an angle ϕ, the moment and force equilibrium equations enable the forming load per unit width, P, to be expressed in terms of the longitudinal and transverse shear viscosities of the material.

$$P = \frac{2\dot{\phi}(\ell_s - \phi(R_r + h))(\eta_L h_L + \eta_T h_T)}{L} \qquad (14)$$

For the case in which the strip possesses no transverse layers (ie. h_T=0), it becomes a simple matter of rearranging equation (14) to yield an expression for the longitudinal viscosity. Once $\eta_L(\phi)$ has been established, the subsequent introduction of transverse layers into the laminated beam may then be used to determine $\eta_T(\phi)$.

Experimental Procedures

The vee-bending experiments were conducted using PLYTRON sheet (a PP/glass fibre unidirectional pre-impregnated material with a nominal 35% fibre volume fraction) consolidated from 8 plies of prepreg. During the course of this study two different lay-up schemes were tested; $[0°]_8$, and $[0°/90°/90°,0°]_S$. In both cases the longitudinal direction was defined to coincide with the control axis (0°), while the transverse direction was defined to coincide with the width as illustrated in Figure 6(a).

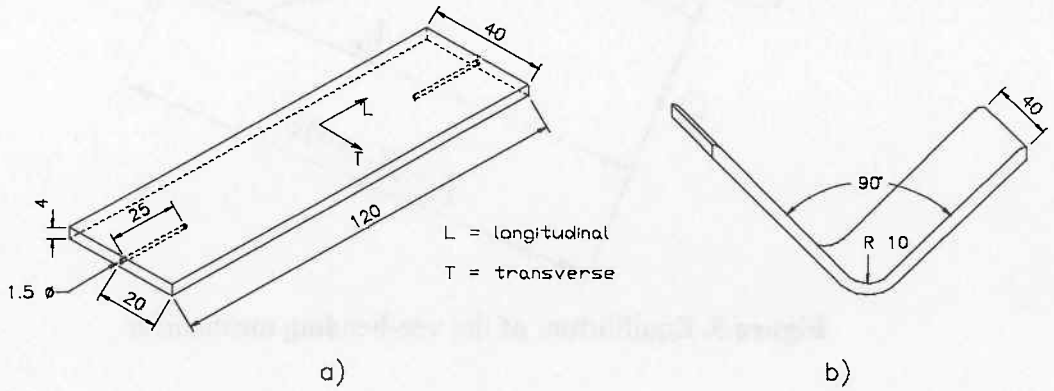

Figure 6. (a) Test sample dimensions, (b) deformed sample.

Experimental Setup

The vee-bending experiments were performed in a benchtop oven which was extensively modified so as to ensure isothermal testing conditions. The oven and bending jig, secured within the oven, were mounted on the crosshead of an Instron 1185 testing machine, capable of the various constant crosshead speeds used in the

experiments. The experiments were also performed over a range of temperatures between 180°C and 150°C. In each test the samples were subjected to a predetermined crosshead displacement which corresponded to a deformed part angle of 90° as shown in Figure 6(b). Forming loads were transferred from the punch to a 50N load cell, positioned above the oven, via a slender stainless steel connecting tube. The analogue load cell output was then amplified before being converted to a digital signal through an A to D circuit board. Load data, sampled at a rate of 5Hz, was then read and recorded on a PC using the LabView™ data acquisition facility. The load data was subsequently analysed using the viscous bending model described in the previous section. Figure 7 shows a schematic representation of the experimental setup.

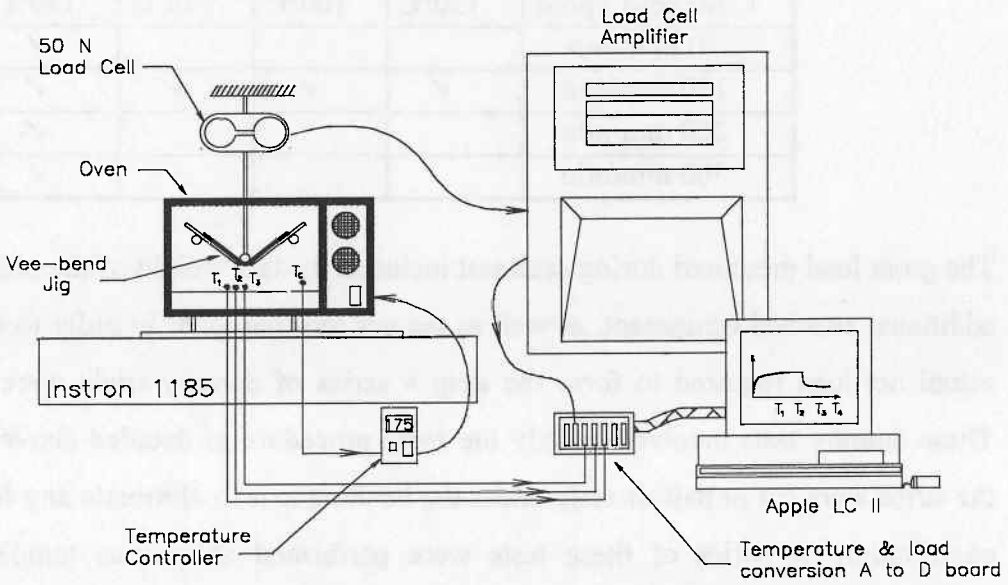

Figure 7. Schematic representation of equipment setup.

The temperature of the oven and sample were controlled by means of a Gefran 1000 PID temperature controller with the feedback provided by one of the two K-type thermocouples embedded at the ends of the sample. By using the self tuning feature of the controller, it was found that the temperature of the sample and testing jig could be controlled to within ±0.5°C of the desired test temperature. In addition, three ancillary thermocouples were attached to various points of the vee-bending jig to monitor the temperature throughout the testing sequence.

As can be seen from Table 1 the tests were performed over a relatively wide range of forming rates and temperatures. For each test the same heating sequence was used, namely the samples were positioned on the platens of the jig with the thermocouples in place and then heated to 185°C. A 5 minute period was then allowed to enable the temperature of the apparatus and sample to stabilise. After this heating and stabilising period the oven temperature was set to the desired test temperature. Upon cooling to the set test temperature the sample was held for a period of time until the temperature stabilised. The actual test then commenced.

Table 1. Outline of testing program.

Crosshead Speed	150°C	160°C	170°C	180°C
50 mm/min				✓
100 mm/min	✓	✓	✓	✓
200 mm/min				✓
500 mm/min				✓

The gross load measured during each test included the tare weight of the platens and the additional attached equipment, as well as the net forming load. In order to establish the actual net load required to form the strip a series of dummy trials were performed. These dummy tests involved exactly the same procedure as detailed above except that the strips were cut in half directly under the bending axis to eliminate any forming load contribution. A series of these tests were performed at various temperatures and crosshead rates. The tare loads measured from the dummy trials were then simply subtracted from the measured gross forming loads obtained in the actual bending tests. Not surprisingly, the temperature was found to have a negligible effect on the measured tare loads.

Description of the Vee-bending Jig

In the bending jig used for this investigation two highly polished platens are mounted on a pair of Teflon™ cams rather than the circular supports used by Mander[6]. This ensures minimal frictional resistance in addition to a constant rate of angular rotation of the platens. A schematic representation of the bending jig is shown in Figure 8. It consists of two rectangular platens hinged together by a pair of swing arms which are

attached to the platens. The platen surfaces are machined flat and highly polished while the swing arms are connected together by means of a hinge pin which enables the platens to "fold" with an action similar to that of a door hinge. The folding action, or rotation, of each platen is manipulated by the pair of cams which have been NC machined in such a way as to ensure that the rate of angular rotation of both platens is constant throughout the deformation. In addition, the platens have parallel grooves machined on their underside to act as guide rails for the cams. To ensure the correct alignment of the platens during the deformation, the hinge pin is constrained to vertical movement by means of the guide slot machined in the side plates.

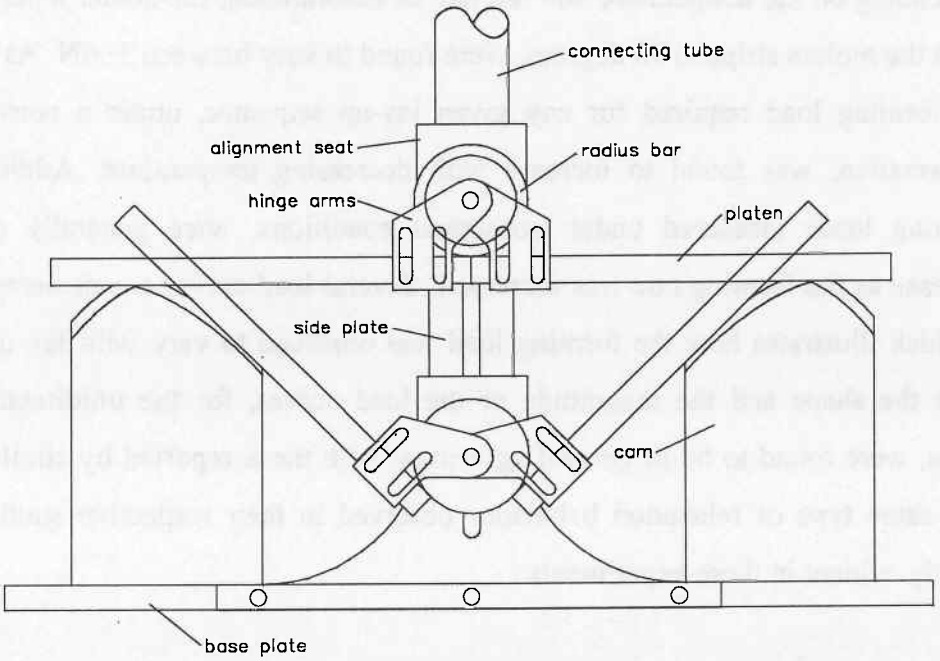

Figure 8. Schematic description of vee-bending Jig showing undeformed and deformed configurations (note that the front side plate is omitted for clarity).

The forming load is transferred from the radius bar through a slender stainless steel tube to a 50N load cell positioned directly above the oven. The radius bar is attached to the connecting tube via a detachable seat arrangement which ensures the correct alignment of the bar and tube. As the seat and radius bar are moved in a relative downward motion (by the moving Instron crosshead) the molten sample is progressively wrapped around the radius bar. The radius bar is prevented from indenting the molten sample as the relative gap between the platens and radius bar is fixed by the length of the radius swing arms. To enforce the plane strain condition, the radius bar has an end plate which

prohibits the molten sample from flowing transversely. A strip of Mylar™ film is placed between the sample and the platens to prevent the molten strip adhering to the polished surface during the test.

Results and Discussion

Before presenting the results pertaining to the materials shear behaviour, it would seem appropriate to initially examine the general form of the load curves obtained in the trials. A notable feature of the experiments was the very small forming loads measured. Depending on the temperature and the rate of deformation, the actual loads required to form the molten strips to 90 degrees, were found to vary between 1~6N. As anticipated, the forming load required for any given lay-up sequence, under a constant rate of deformation, was found to increase with decreasing temperature. Additionally, the forming loads measured under isothermal conditions, were generally observed to increase as the forming rate was increased. Several load curves are presented in Figure 9 which illustrates how the forming load was observed to vary with lay-up sequence. Both the shape and the magnitude of the load curves, for the unidirectional ($[0°]_8$) strips, were found to be in general agreement with those reported by similar studies[5,6]. The same type of relaxation behaviour observed in their respective studies was also clearly evident in these experiments.

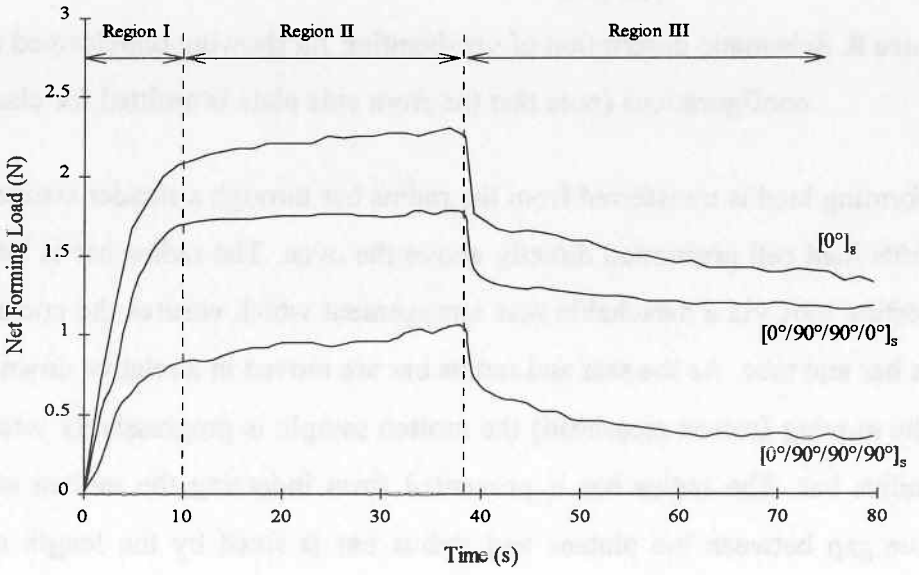

Figure 9. Net forming loads plotted as a function of time for various lay-ups; forming rate 100mm/min, temperature = 180°C.

In general the net forming load curves for all the samples tested could be divided into three regions as shown in Figure 9. Region I indicates the initial loading part, and the second definable zone (Region II) is characterised by a gradually increasing load up to the point at which the crosshead is stopped. Region III begins as the test is completed and is characterised by an instantaneous drop in load followed by an asymptotic decay with time. It should be noted that the material exhibits visco-elastic behaviour which is not entirely compatible with the viscous bending model used in this study, but useful viscosity results can be determined from the loading as will be shown later.

The attention will now be focused on the more important task of interpreting the material's longitudinal and transverse shear behaviour from these forming load curves. For a laminated strip possessing both longitudinal and transverse layers, initially it is necessary to establish η_L as a function of ϕ. In order to achieve this, an initial set of vee-bending experiments were performed on strips possessing no transverse layers (ie. $[0°]_8$ samples), thus eliminating η_T from equation (14). The results of these tests are presented in Figure 10 for the case in which the temperature is maintained at 180°C for various rates of deformation. Similar results were established for the case in which the forming rate was kept constant and the temperature varied between 180°C and 150°C.

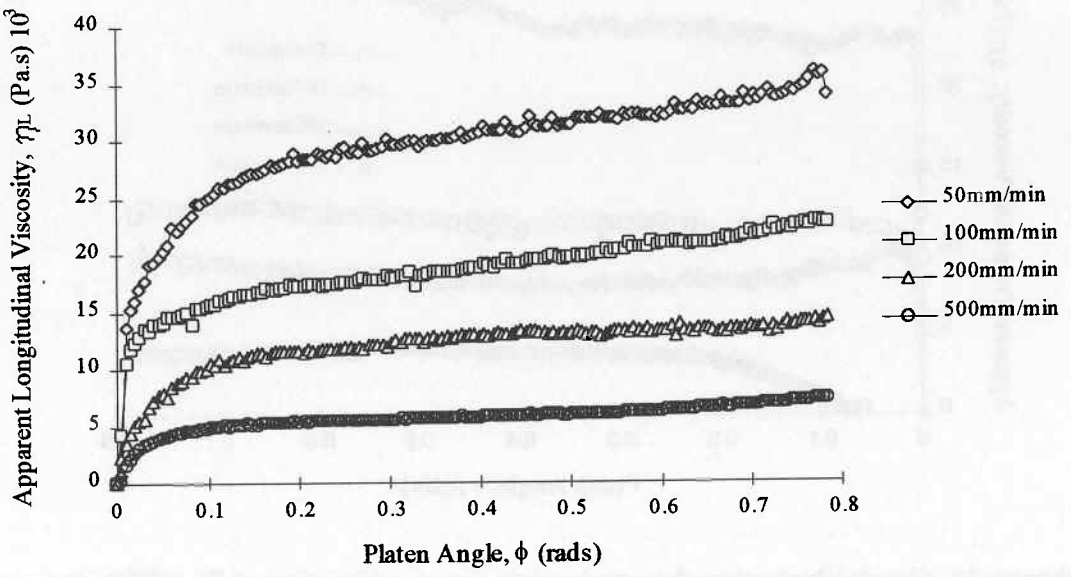

Figure 10. Graph illustrating the apparent longitudinal viscosity of PLYTRON at various rates of deformation; temperature = 180°C.

At 180°C a noticeable shear thinning effect is evident as the apparent longitudinal viscosity is observed to decrease with increasing rates of deformation. This shear thinning trend, depicted in Figure 10, is in qualitative agreement with that observed by other researchers[4,5,6].

Having established η_L as a function of ϕ, over a variety of forming rates and temperatures, allows the analysis of the transverse shear behaviour to be undertaken. The method employed to do this was identical to that used for establishing η_L; however, it required that transversely orientated layers be introduced to the laminated strip. As expected, the forming loads obtained in this series of tests were found to be consistently lower than those measured for the uni-directional laminates at the same forming rate and temperature. Figure 11 shows the apparent transverse viscosity of PLYTRON as a function of platen angle for various forming rates. The initial part of the curves may be ignored due to the transitional behaviour previously mentioned. A similar shear thinning trend to that observed in the longitudinal behaviour is also evident in the transverse shear response. This non-linear behaviour is supported by Groves *et al.*[4] who applied oscillatory shear techniques to determine both the longitudinal and transverse shear behaviour of a similar material.

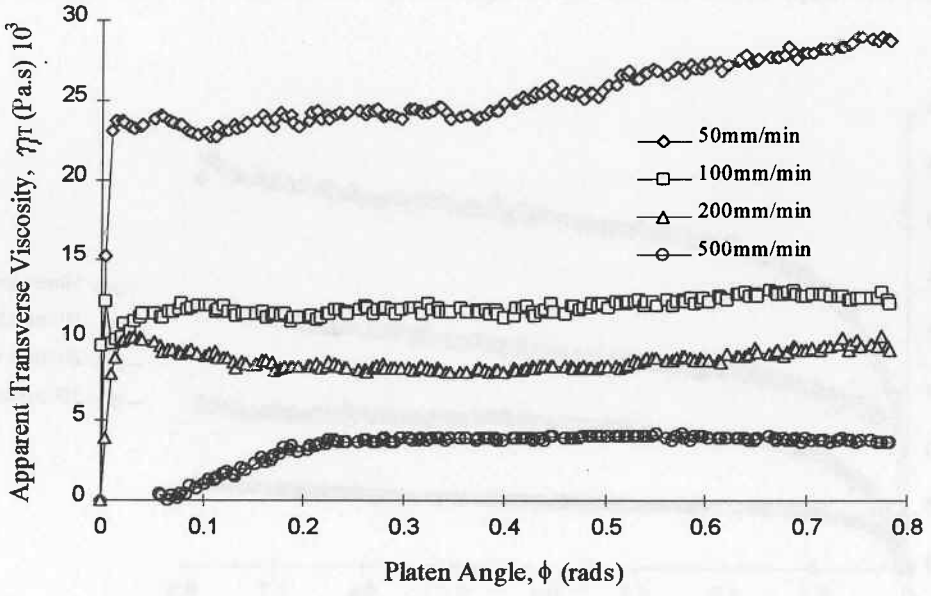

Figure 11. Graph illustrating the apparent transverse viscosity of PLYTON for various rates of deformation; temperature = 180°C.

Figure 12 shows how the apparent transverse viscosity of PLYTRON was found to vary with forming temperature. The variability in η_T with forming angle at 160°C and 150°C reflects the degree of elasticity retained within the material at lower forming temperatures. The same trend was also evident in the longitudinal shear response at lower forming temperatures, thus demonstrating that a viscous model is perhaps only applicable at temperatures well inside or above the molten range of the polymer matrix.

The results obtained to this point allow a direct comparison to be made between the transverse and longitudinal shear viscosities. This provides an important opportunity to verify a number of theoretical models which have been proposed in an attempt to relate η_T and η_L to the fibre volume fraction f and the matrix viscosity η_M. A summary of the models that have been proposed by Pipes[11], Christensen[12], and Binding[13] is given in Table 2. These models are based around geometric arguments and assume somewhat of an idealised behaviour. The models of Pipes and Christensen predict that $\eta_T > \eta_L$ for all fibre volume fractions, while the model of Binding predicts only η_L as a function of f and η_M. Furthermore, the longitudinal viscosity, as predicted by Binding, is larger than either of the transverse viscosity terms predicted by Pipes and Christensen.

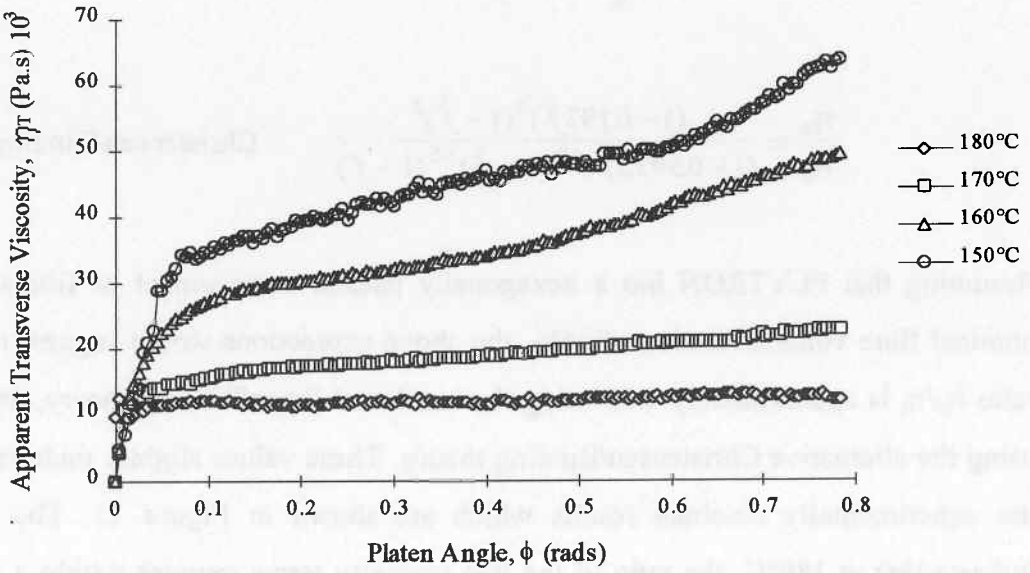

Figure 12. Graph illustrating the apparent transverse viscosity of PLYTON for various forming temperatures; forming rate = 100mm/min.

Table 2. Theoretical models relating η_T and η_L to the fibre volume fraction f and η_M.

	η_T/η_M	η_L/η_M
Pipes[11]	$\frac{1}{1-\sqrt{\hat{f}}}$	$\frac{2-\sqrt{\hat{f}}}{2(1-\sqrt{\hat{f}})}$
Christensen[12]	$\frac{(1-0.193\hat{f})^3}{(1-0.5952\hat{f})^{3/2}(1-\hat{f})^{3/2}}$	$\frac{1+0.873\hat{f}}{(1-0.8815\hat{f})^{1/2}(1-\hat{f})^{1/2}}$
Binding[13]	-	$\frac{1-f}{(1-\sqrt{\hat{f}})^2}$

$\hat{f} = 2\sqrt{3}f/\pi \ (0 \leq f \geq \pi/(2\sqrt{3}))$

It is to be noted that the viscosity results obtained for PLYTRON indicate that $\eta_T < \eta_L$ for all the temperatures and forming speeds investigated, which is clearly not in agreement with the models of Pipes and Christensen. However, it is interesting to note that by combining the model of Binding with those of Pipes and Christensen to eliminate the matrix viscosity, expressions for the viscosity ratio η_T/η_L may be obtained which are in line with the experimentally observed results:

$$\frac{\eta_T}{\eta_L} = \frac{1-\sqrt{\hat{f}}}{1-f} \qquad \text{Pipes/Binding}$$

$$\frac{\eta_T}{\eta_L} = \frac{(1-0.193\hat{f})^3(1-\hat{f})^2}{(1-0.5952\hat{f})^{3/2}(1-\hat{f})^{3/2}(1-f)} \qquad \text{Christensen/Binding}$$

Assuming that PLYTRON has a hexagonally packed arrangement of fibres and a nominal fibre volume fraction of 35%, the above expressions would suggest that the ratio η_T/η_L is approximately 0.58 using the combined Pipes/Binding theory, and 0.54 using the alternative Christensen/Binding theory. These values slightly underestimate the experimentally obtained results which are shown in Figure 13. The results indicate that at 180°C, the ratio of the two viscosity terms remains within a narrow band for the various deformation rates studied in this investigation. This is in

agreement with the idealised theory presented above, in which no rate dependent terms arise. The results would also tend to suggest that the shear thinning behaviour observed in both the longitudinal and transverse directions, is largely attributable to the non-linear behaviour of the molten matrix material. It should be noted that the idealised models presented in Table 2 fail to adequately take account of the resin rich layers that form between the individual plies. It is the authors' belief that the presence of these thin layers, coupled with a slight amount of fibre misalignment, which accounts for the discrepancy between the theoretical and actual results.

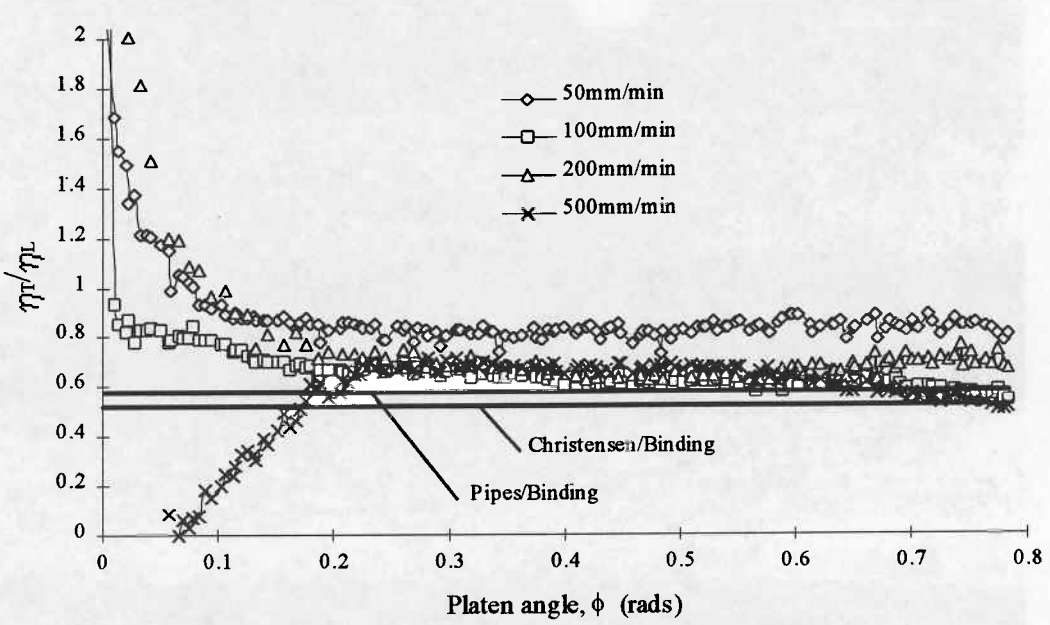

Figure 13. Transverse to longitudinal viscosity ratios for various forming rates; temperature = 180°C.

Finally, it is important to revisit the viscous bending model and address some of the assumptions involved in its development. The bending model presented earlier assumed the transversely orientated layers to behave kinematically, in an identical manner to that of the adjacent longitudinal layers. The validity of this assumption can be assessed by considering the thickness of the transverse layers, which should, according to the model, remain constant through the entire deformation. In order to gauge the thickness variation in these layers a number of deformed samples were cut, polished, and examined using an optical microscope. As shown in Figure 14, the

thickness variation in the transverse layers, recognisable by their specular appearance, was found to be negligible in the $[0°/90°/90°/0°]_s$ samples. However, a number of tests performed on $[0°/90°/90°/90°]_s$ samples revealed a significant transverse thickness variation of up to 15% through the length of the samples. The application of the model should therefore be restricted to the bending of laminates which at least possess transverse layers of total thickness comparable to that of the adjacent longitudinal layers. The extent to which the thickness of the transverse layers may be increased, without violating the assumption, remains to be established.

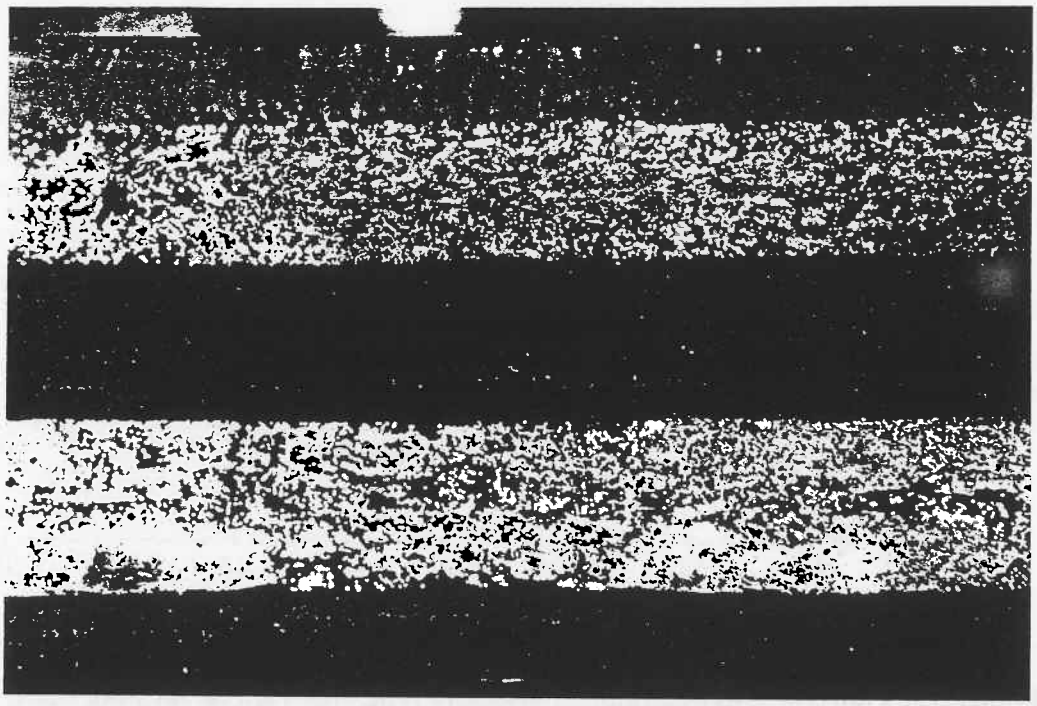

Figure 14. The cross section of a deformed sample $[0°/90°/90°/0°]_s$.

Conclusions

Both the longitudinal and transverse shear behaviours of PLYTRON have been investigated using a novel vee-bending device. The unique design of the bending mechanism is such that it ensures a constant, definable rate of shear deformation through the thickness of a laminated strip, thus allowing both the longitudinal and transverse shear response of the material to be studied.

A laminated viscous bending model has been developed which provides the framework for interpreting the longitudinal and transverse shear behaviour of continuous fibre reinforced thermoplastic materials. The model itself yields an analytical expression relating the load required to bend a laminated strip to the forming geometry, rate of deformation, and the material properties, η_L and η_T.

This study has identified vee-bending as a simple and useful way of determining the longitudinal and the transverse shear behaviour of continuous fibre reinforced thermoplastics. The results of the bending tests indicate that the longitudinal viscosity of PLYTRON is greater in magnitude than the transverse viscosity over the entire range of forming rates and temperatures investigated in this study. Both η_L and η_T were found to exhibit shear thinning behaviour at 180°C, as both terms were observed to decrease in magnitude as the effective shear rate was increased.

The transverse viscosity of PLYTRON was found to vary with both forming rate and temperature. At 180°C, η_T was observed to decrease as the effective shear rate was increased. For the forming rates used in the study, this resulted in a variation of between 30,000 and 4,000 Pa.s. As the forming temperature was lowered a similar increase in η_T was observed. At 150°C a large amount of variation in η_T with forming angle was noticeable thus reflecting the materials increasing elasticity at lower forming temperatures.

The viscosity results obtained from the bending tests have been compared to a number of existing theoretical models which relate η_L and η_T to the fibre volume fraction and the matrix viscosity. The results obtained by using the vee-bend test and viscous theory appear to disagree with the individual models of Pipes and Christensen by predicting $\eta_T < \eta_L$ for all the forming speeds and temperatures investigated. However good correlation is found to exist between the determined viscosity ratios (η_T/η_L) and those achieved by combining the models of Binding and Pipes or Christensen. As predicted by the combined models, the ratios determined by the present method also appear to remain within a narrow band over a relatively wide range of deformation rates.

Acknowledgments

The authors would like to thank the Foundation for Research, Science and Technology (NZ) for their financial support, and the technical staff of the Mechanics of Materials laboratory for their assistance with the experiments. The free supply of material from Borealis (NORWAY) and Mitsui-Toatsu (JAPAN) is also gratefully acknowledged.

References

1. Offringa, A. R. 'Industrial Report: Thermoplastic composites - rapid processing applications', Composites: Part A, 27A, pp. 329-336 (1996).

2. Spencer, A.J.M. 'Deformations of Fibre-Reinforced Materials', Clarendon Press, Oxford, (1972).

3. Goshawk, J.A. and Jones, R.S. 'Structural Reorganisation in the Rheological Characterisation of continuous fibre-reinforced composites in plane shear', Composites: Part A, 27A, pp. 279-286 (1996).

4. Groves, D.J., Stocks, D.M. and Bellamy, A.M. 'Isotropic and anisotropic shear flow in continuous fibre thermoplastics', *Proc. Golden Jubilee meeting of the British Society of Rheology and Third European Rheology Conference*, Edinburgh, UK, pp. 190-192 (1990).

5. Martin, T.A., Bhattacharyya, D. and Collins, I.F. 'Bending of Fibre-Reinforced Thermoplastic Sheets', Composites Manufacturing, 6, pp. 177-187 (1995).

6. S. J. Mander 'Roll Forming of Fibre-Reinforced Thermoplastic Composites', PhD thesis submitted, University of Auckland, New Zealand (1996).

7. Pipkin, A.C. and Rogers, T.G. 'Plane Deformations of Incompressible Fibre-Reinforced Materials', Journal of Applied Mechanics, Vol. 38, Trans. ASME, Vol. 93, Series E, pp. 634-640 (1971).

8. Rogers, T.G. 'Rheological Characterisation of Anisotropic Materials', Composites, Vol. 20 (1), pp. 21-27 (1989).

9. Rogers, T.G. and Pipkin, A.C. 'Small Deflections of Fibre-Reinforced Beams or Slabs', Journal of Applied Mechanics, Trans. ASME, pp. 1047-1048 Dec. (1971).

10. Spencers, A.J.M. 'Plane Strain Bending of Laminated Fibre-Reinforced Plates', Quarterly Journal of Mechanics and Applied Mathematics, Vol. 25, Part 3, pp. 387-400 (1972).

11. Pipes, R.B. 'Anisotropic viscosities of an orientated fibre composite with power-law matrix', Journal of Composite Materials, Vol. 26, pp. 1536-1552 (1992).

12. Christensen, R.M. 'Effective viscous flow properties for fibre suspensions under concentrated conditions', Journal of Rheology, 37, pp. 103 - 121 (1993).

13. Binding, D.M. 'Capillary and contraction flow of long (glass) fibre filled polypropylene', Composites Manufacturing, 2, pp. 243-252 (1991).